Z_2 Monopoles, Vortices, and The Deconfinement Transition in Mixed Action SU(2) Gauge Theory

Saumen Datta[*]

The Mehta Research Institute of Mathematics and Mathematical Physics, Chhatnag Road, Jhusi, Allahabad 211019, India

R. V. Gavai[†]

Department of Theoretical Physics,Tata Institute of Fundamental Research, Homi Bhabha Road, Mumbai 400005, India

Abstract

Adding separate chemical potentials λ and γ for Z_2-monopoles and vortices respectively in the Villain form of the mixed fundamental-adjoint action for the SU(2) lattice gauge theory, we investigate their role in the interplay between the deconfinement and bulk phase transitions using Monte Carlo techniques. Setting λ to be nonzero, we find that the line of deconfinement transitions is shifted in the coupling plane but it behaves curiously also like the bulk transition line for large enough adjoint coupling, as for $\lambda = 0$. In a narrow range of couplings, however, we find separate deconfinement and bulk phase transitions on the same lattice for nonzero and large λ, suggesting the two to be indeed coincident in the region where a first order deconfinement phase transition is seen. In the limit of large λ and γ, we obtain only lines of second order deconfinement phase transitions, as expected from universality.

PACS code: 11.15.Ha,12.38.Aw

Typeset using REVTEX

[*]E-mail:saumen@mri.ernet.in

[†]E-mail:gavai@theory.tifr.res.in

I. INTRODUCTION

The continuum limit of a lattice regularized gauge theory is defined at its critical point where the lattice correlation length is infinite. One therefore expects that a large number of lattice actions, differing from each other by only irrelevant terms in the sense of the renormalization group, describe the same continuum physics.

For pure gauge theories, the simplest discretized action, the Wilson action [1], is widely used in both analytical and numerical studies. It has been very successful in revealing several nonperturbative features of gauge theories. Most such investigations are, however, necessarily carried out for a finite value of the lattice spacing a. It seems therefore imperative that the universality of these results is verified by employing other forms of lattice actions. Such a study of the universality of the deconfinement transition for SU(2) gauge theory was initiated in Ref. [2] for the Bhanot-Creutz action [3]

$$S_{BC} = \beta_f \sum_p \left(1 - \frac{1}{2}\mathrm{Tr}_f U_p \right) + \beta_a \sum_p \left(1 - \frac{1}{3}\mathrm{Tr}_a U_p \right) , \qquad (1)$$

where the summation runs over all the plaquettes of the lattice and the subscript, $f(a)$ indicates that the trace is taken in the fundamental (adjoint) representation. The Wilson action corresponds to setting $\beta_a = 0$ in Eq. (1). It has a second order deconfinement phase transition at which the order parameter $\langle |L_f| \rangle$ acquires a nonzero value, where

$$L_f(\vec{x}) = \frac{1}{2}\mathrm{Tr}_f \prod_{\tau=1}^{N_\tau} U_\tau(\vec{x}, \tau) , \qquad (2)$$

and U_τ are the gauge fields in the time direction. The finite size scaling analysis [4] of its susceptibility, $\chi_{|L_f|} = \langle L_f^2 \rangle - \langle |L_f| \rangle^2$, yielded an exponent $\omega = 1.93 \pm 0.03$, in good agreement with the corresponding value (1.965±0.005) for the three dimensional Ising model. Universality of the continuum limit predicts a similar deconfinement transition belonging to the same universality class as the three dimensional Ising model for all values of β_a.

Monte Carlo simulations for Eq. (1) on $N_\sigma^3 \times N_\tau$ lattices with $N_\tau = 4$ showed [2] that while the second order deconfinement transition point for the $\beta_a = 0$ Wilson action entered the $\beta_f - \beta_a$ plane as a line of second order transitions, the transition, surprisingly, turned first order for large enough β_a. This was evident from the facts that i) the order parameter, $\langle |L_f| \rangle$, became nonzero discontinuously at the transition and ii) the exponent of its susceptibility changed from the Ising model value to 3. If the change of the order of the deconfinement transition were to persist in the continuum limit, it would be a serious violation of universality. On the other hand, the deconfinement line was also found to coincide with the known bulk transition line [3] for $N_\tau = 4$. Studies with varying N_τ further revealed that it scarcely moves as one increases N_τ, especially in the region where a strong first order deconfinement transition is observed [5].

Similar results were also obtained [6] in studies with a Villain form of the mixed fundamental-adjoint action [7],

$$S = \beta_f \sum_p \left(1 - \frac{1}{2}\mathrm{Tr}_f U_p \right) + \beta_v \sum_p \left(1 - \frac{1}{2}\sigma_p.\mathrm{Tr}_f U_p \right), \qquad (3)$$

where σ_p are auxiliary Z_2 variables defined on the plaquettes and the partition function has a sum over all possible values of the σ_p variables. This summation ensures that the second term gets contributions only from the integer representations of SU(2). The deconfinement phase transition in the β_f - β_v plane of this action was shown [6] to have similar features as above : the deconfinement transition turned first order for large enough β_v and the transition line merged with the known bulk transition line for this action [7].

Another example of similar interplay of bulk and deconfinement effects was shown [8,9] to be the SO(3) lattice gauge theory, i.e, for β_f =0 in Eqs. (1) and (3). Being in the same universality class, it should also have a second order deconfinement phase transition, although it does not have an order parameter like the SU(2) theory. The only transition found in Refs. [8,9] for different N_τ coincided with the known first order bulk transition.

One way the above conflicting indications can be interpreted is to postulate that the bulk transition interferes with the deconfinement line in such a manner as to make the two lines coincident for a substantial range of N_τ and couplings for all the above actions. A possible way to test this hypothesis is to modify these actions further by such additional irrelevant term(s) that the bulk transitions are either shifted in the coupling plane or entirely eliminated. The bulk transition in the Villain form of the SO(3) gauge theory is known to be caused by a condensation of Z_2 monopoles in the strong coupling phase [10]. These monopoles are absent in the weak coupling region, and can be suppressed at stronger couplings by adding an irrelevant term to the action. Investigations [11] of the monopole suppressed theory at finite temperature found a continuous deconfinement transition, very similar to the transition for the SU(2) theory with Wilson action. This suggests trying an extension of the technique of suppression of bulk transitions to the mixed actions as well. For the action in Eq. (3), the bulk transitions are caused by the Z_2 monopoles and vortices [7]. In this work, we study its finite temperature phase diagram with suppression of these objects.

The plan of our paper is as follows. In the next section, we review briefly the bulk phase diagram for the action (3) and the results of studies of deconfinement transition for it. Following the SO(3) results, we suppressed only the Z_2 monopoles for it and studied the resulting theory in the β_f - β_v plane. As seen in Sec. III, this resulted in suppression of the bulk transition line coming from the SO(3) axis, but it was found inadequate for suppressing the remaining bulk transition line, where again the same interplay of bulk and deconfinement effects was seen. Nevertheless, we were able to demonstrate that a second order deconfinement phase transition and a first order bulk transition *both* exist on the *same* lattice but at different locations in a small range of β_v. In Sec. IV, we added an additional term to suppress the Z_2 vortices. This resulted in a complete elimination of all the bulk lines and a universal deconfinement transition in the entire β_f - β_v plane was found. A summary of our results and our conclusions are presented in Sec. V.

II. PHASE DIAGRAM FOR MIXED VILLAIN ACTION

The phase diagram of the mixed Villain action, Eq. (3), was studied in Ref. [7] on symmetric lattices and was found to be qualitatively similar to that for the Bhanot-Creutz action, Eq. (1). As shown in Fig. 1, lines of first order transition, emanating from the $\beta_v \rightarrow \infty$ region and the $\beta_f = 0$ axis, join, and extend to the low β_v phase, before ending

at $\beta_v \approx 2.2$. The bulk transitions in this action can be understood to be due to certain Z_2 topological objects. Defining the monopole density, M, and the electric current density, E, as

$$M = 1 - \left\langle \frac{1}{N_c} \sum_c \sigma_c \right\rangle \quad \text{with} \quad \sigma_c = \prod_{p \in \partial c} \sigma_p$$

$$\text{and} \quad E = 1 - \left\langle \frac{1}{N_l} \sum_l \sigma_e \right\rangle \quad \text{with} \quad \sigma_e = \prod_{p \in \hat{\partial} l} \sigma_p \tag{4}$$

where N_c and N_l are the number of elementary cubes and links of the lattice, respectively, the bulk phases are characterized by presence of condensates of these objects [7]. The strong coupling phase has both E and M nonzero, corresponding to condensation of both Z_2 electric vortices and magnetic monopoles, while the large β_f and β_v phase, relevant for the continuum limit, is free of both condensates, as summarized in Fig. 1 (~ 0 in the figure means zero up to $O(\exp(-\beta_f))$).

The finite temperature phase transitions for this theory have been explored in Ref. [6]. As mentioned in Sec. I, the results are similar to those obtained in Refs. [2,5] for the Bhanot-Creutz action. The second order finite temperature transition line, coming out of the $\beta_v = 0$ axis, turns first order and joins the bulk transition line at its endpoint [12]. The finite temperature transition on the β_v axis was studied in Ref. [9]. It was found to be a coincident bulk and deconfinement transition for $N_\tau = 4$, 6 and 8 lattices. Since the bulk transition on the β_v axis is due to the melting of the monopole condensate present in the strong coupling phase (Fig. 1), and since the monopoles are not present in continuum limit, we studied the deconfinement transition on this axis after suppressing the monopoles [11]. The resulting theory i) had no bulk transitions, ii) yielded a deconfinement transition very similar to that found for the Wilson action, in agreement with expectations based on universality and iii) displayed a shift in the transition point with N_τ. As a natural next step, we turn to a study of the mixed theory (action (3)) with monopole suppression, as described below.

III. PHASE DIAGRAM WITH MONOPOLE SUPPRESSION

Adding a chemical potential term for the monopoles as in Ref. [11], the mixed fundamental-adjoint Villain action becomes

$$S(U, \sigma) = \beta_f \sum_p \left(1 - \frac{1}{2} \text{Tr}_f U_p \right) \tag{5}$$

$$+ \beta_v \sum_p \left(1 - \frac{1}{2} \sigma_p . \text{Tr}_f U_p \right) + \lambda \sum_c (1 - \sigma_c) \, ,$$

where the last summation runs over all the elementary 3-cubes of the lattice, and σ_c is defined in Eq. (4). The classical continuum limit is left unaffected by the additional monopole term and one obtains the same continuum relation, $4g^{-2} = \beta_f + \beta_v$, in that limit. For SO(3), $\lambda = 1$ was found to be sufficient to suppress the bulk transition. We therefore took $\lambda = 1$ for our simulations in the entire β_f - β_v plane. Our simulations consisted of a 3-steps iteration. First, all the gauge variables were updated using Creutz's heatbath algorithm. This was followed

by a heatbath sweep for the Z_2 variables. In the third step of our iteration, a fraction of the links (arbitrarily chosen to be $\frac{1}{4}$) were multiplied by a Z_2 element subject to a probability determined by the β_f term. This third step is essential for reducing the otherwise enormous autocorrelations for large λ simulations, and generalizes the similar step used in Ref. [11] for the SO(3) gauge theory. Measurements were made after every such compound iteration. Using hysteresis runs of 15000 iterations per point, and monitoring the plaquette variables $P = \langle \frac{1}{2} \mathrm{Tr}_f U_p \rangle$ and $P_a = \langle \frac{1}{2} \sigma_p \mathrm{Tr}_f U_p \rangle$, we mapped out the phase diagram on an $8^3 \times 4$ lattice.

First order transitions, with significant discontinuities in the average plaquette P for $\beta_v > \beta_f$ and the "adjoint" plaquette P_a for $\beta_v < \beta_f$, were observed. The transition points are shown by filled circles in Fig. 2. While the transition line in the large β_v region is very similar to the $\lambda = 0$ case (Fig. 1), unlike that case the transition line does not have an endpoint and divides the $\beta_f - \beta_v$ plane in two disjoint parts. Also the transition line coming out of the $\beta_f = 0$ axis in Fig. 1 is absent here. Since it is caused by condensation of monopoles, which have been suppressed here, its absence was to be expected.

To look for the deconfinement transition, we monitored the behavior of $\langle |L_f| \rangle$. The deconfinement transition point on the Wilson axis was seen to extend into a line of continuous deconfinement transitions as we switched on β_v. On increasing β_v, the deconfinement transition line was seen to merge with the first order line, and the order parameter $\langle |L_f| \rangle$ showed a discontinuous jump to a nonzero value, indicating a first order deconfinement transition for these points. The dotted (solid) line in Fig. 2 shows the line of second (first) order deconfinement transitions. The facts that unlike the $\lambda = 0$ case, the 1st order line does not have an endpoint here, and the line coming from the large β_f side is clearly not a deconfining line before the line coming from the Wilson axis meets it at $\beta_f \sim 2$, give credence to the hypothesis that the line in the large β_v region is a coincident bulk and deconfinement transition line and, as we will see later, allows one to actually see two separate transitions on the same lattice. In what follows, we discuss first the 1st order transition line and then the deconfinement transition line in some more detail.

A. The 1st Order Transition Line

The first order transition points, shown in Fig. 2, are listed in Table I along with the discontinuities in various observables and the values of $\langle |L_f| \rangle$ at the transition point on the low β_f (β_v) side at fixed β_v (β_f). In the $\beta_v > \beta_f$ region, the transition is associated with large discontinuities in P and $\langle |L_f| \rangle$. Also $\langle |L_f| \rangle \sim 0$ till the transition point, indicating that the transition line signals a deconfinement transition. The transition line in the large β_v region is very similar to the $\lambda = 0$ case. This is expected, since in the large β_v limit, the monopoles are automatically suppressed(see Fig. 1) and the additional monopole suppression term does not have much effect. As $\beta_v \to \infty$, the dominant contribution to the path integral comes from those configurations which have $\sigma_p . \mathrm{Tr}_f U_p = 2$. Now the plaquette variables σ_p can be integrated out, constraining the gauge variables U_l to take values only in the center group $Z_2 : \sigma_p = \frac{1}{2} \mathrm{Tr}_f U_p = \prod_{l \in \partial p} \sigma_l$ where σ_l are Z_2 variables defined on the links and the U_l are frozen to the values σ_l. Then $\sigma_c = 1$ for all cubes c in this limit, and therefore the additional monopole suppression term does not have any effect. The action reduces to that of the Z_2 gauge theory, which has a well known first order transition at $\beta_f \approx 0.44$ with a discontinuity in the average plaquette. As β_v is reduced from ∞, the transition line starts

shifting from that of the $\lambda = 0$ case. The transition line shown in Fig. 2 can be reproduced reasonably well up to $\beta_v \sim 2$ by taking into account only configurations where U_l can have small fluctuations around σ_l:

$$U_l = \sigma_l U_l' \quad \text{where } U_l' = 1 + igA_l \ .$$

Perturbatively integrating over the fluctuations yield, in the leading order,

$$P_a = \frac{1}{2}\langle \sigma_p \text{Tr}_f U_p \rangle = 1 - \frac{3}{4\beta_f} + O(\frac{1}{\beta_f^2}) \ .$$

Up to this order, the integral over A_l only produces a renormalization of β_f, and the transition point changes to

$$\beta_f \approx \frac{0.44}{\left(1 - \frac{3}{4\beta_v}\right)} \ . \tag{6}$$

The prediction of Eq. (6), shown in Fig. 2, matches the Monte Carlo results quite well for $\beta_v \gtrsim 2$.

In the large β_f region, the transition is associated with a large discontinuity in P_a, as can be seen from Table I. Also from the $\langle |L_f| \rangle$ value at the lower side of the transition point one can see that both the sides of the transition are in deconfined state. The transition line in this region can be understood from the known bulk transition in the Z_2 gauge-Higgs theory. In the $\beta_f \to \infty$ limit, the gauge variables are frozen : $\text{Tr}_f U_p = 2 \ \forall p$. The action in Eq. (5) then reduces to

$$S = \beta_v \sum_p (1 - \sigma_p) + \lambda \sum_c (1 - \sigma_c) \ , \tag{7}$$

after dropping an irrelevant constant. It describes a system with only Z_2 degrees of freedom σ_p. Under a duality transformation [13], one can rewrite it as the action for a Z_2 gauge-Higgs system (modulo irrelevant constants):

$$\tilde{S} = -\tilde{\beta}_v \sum_p \prod_{l \in \partial p} \gamma_l - \tilde{\lambda} \sum_{i,\mu} s_i \gamma_{i,i+\mu} s_{i+\mu} \ . \tag{8}$$

Here s and γ are Z_2 variables residing on the sites and links of the dual lattice respectively, and

$$\left.\begin{array}{c} \tilde{\beta}_v \\ \tilde{\lambda} \end{array}\right\} = \frac{1}{2} \ln \ \coth \left\{ \begin{array}{c} \beta_v \\ \lambda \end{array} \right. . \tag{9}$$

The Z_2 gauge-Higgs system is known to have a nontrivial phase diagram [14], leading to a nontrivial structure in the β_v - λ plane at $\beta_f = \infty$ for the mixed Villain action. For $\lambda = 1$, a first order transition at $\beta_v \approx 0.44$ is predicted for $\beta_f = \infty$. For large but finite β_f, the gauge variables fluctuate around the frozen value and yield the leading order estimate for the transition point,

$$\beta_v \approx \frac{0.44}{\left(1 - \frac{3}{4\beta_f}\right)} \ . \tag{10}$$

6

This leading order estimate is seen in Fig. 2 to work quite well up to $\beta_f \sim 2$. It is also consistent with Table I, which shows the transition to have a nearly continuous P and an almost constant discontinuity in P_a in the region of very large β_f.

While the above effective descriptions of the bulk transitions for $\beta_f \to \infty$ and $\beta_v \to \infty$ were different, they are probably related by a duality transformation. In the $\lambda \to \infty$ limit, the theory is self-dual [15]. In this limit σ_c is constrained to be 1, which can be solved as $\sigma_p = \prod_{l \in p} \sigma_l$, where σ_l are Z_2 variables defined on links. Now a transformation $U_l \to U_l \sigma_l$ interchanges the role of the fundamental and adjoint terms, leaving the action invariant. Under this duality transformation, $\beta_f \leftrightarrow \beta_v$ and $P \leftrightarrow P_a$. Even for $\lambda = 1$, the constraint $\sigma_c = 1$ is approximately true, and the self-duality is approximately obeyed. The locations of first order transition points in Fig. 2 and the discontinuities in the plaquette variables P and P_a presented in Table I, display such a symmetry around the $\beta_f = \beta_v$ line. Taken together with the good agreement of Eqs. (6) and (10) with the Monte Carlo results in Fig. 2, it leads one to the identification of the entire first order transition line traced out by the data points as a bulk transition line. Since the order parameter for the deconfinement phase transition, $\langle |L_f| \rangle$, becomes nonzero on the same line for $\beta_v \gtrsim 0.74$, one has a coincident deconfinement transition line as well. To investigate the origin of the deconfining nature of the first order line for $\beta_v \gtrsim 0.74$, we next turn to an exploration of the deconfinement line starting from the small β_f side.

B. The 2nd Order Transition Lines

For $\beta_v = 0$, the chemical potential term decouples from the SU(2) part and we have the usual Ising-like second order deconfinement transition on this axis, at $\beta_f \approx 2.3$ for $N_\tau = 4$ lattices [4]. One expects, from continuity, a second order transition also for small β_v, as in all the examples mentioned in Sec. I. Hysteresis runs at $\beta_v = 0.3$, 0.5 and 0.7 did indeed indicate a continuous deconfinement transition. For a more quantitative study, we studied the $|L_f|$-susceptibility, $\chi_{|L_f|}$, on $N_\sigma^3 \times 4$ lattices at each β_v with $N_\sigma = 8$, 12 and 16. For each lattice, a low statistics run was made at the transition point estimated from hysteresis runs, and the peak of the susceptibility estimated by extrapolating to nearby couplings using Ferrenberg - Swendsen methods [16]. If the peak was not too far from the input β_f, a longer run was made to generate 10^5 configurations. Otherwise the procedure was repeated at the fresh peak location. The susceptibility curves for the three β_v values are shown in Fig. 3. The critical exponent ω at each β_v, obtained from a linear fit to $\ln (\chi_{|L_f|})_{max} = \omega \ln N_\sigma$, is shown in Table II and is seen to be in good agreement with the $\beta_v = 0$ exponent. The average plaquette P from these runs was smooth everywhere, and the corresponding susceptibility peaks did not sharpen with N_σ at all, indicating a lack of bulk transition at these points. The transition points, shown in Fig. 2 by triangles, are therefore pure finite temperature transitions.

On increasing β_v further, the transition was found to change its behavior. Already at $\beta_v = 0.74$, the rise of Polyakov loop from zero was associated with a discontinuity, indicating a first order deconfinement transition. The first order nature of the transition at this coupling was ascertained by a finite size scaling study. The distribution of the plaquette and Polyakov loop variables at the transition point are shown in Fig. 4. They show the presence of metastable states, and with increase of spatial lattice size, the two - peak structure was seen

to sharpen further without any visible movement in the peak positions, indicating a first order transition in the infinite volume limit. Fig. 4 also clearly shows that the transition is a deconfining one, since the L_f distribution at the lower state is peaked about zero.

On increasing β_v further, the same behavior continued : the deconfinement transition line, characterized by rise of $\langle |L_f| \rangle$ from ~ 0 to a nonzero value, was associated with a discontinuous jump. Also the average plaquette displayed a discontinuity at the same point. In Fig. 2 the complete deconfinement line is shown with the dotted part indicating second order and the solid part indicating first order transitions. This line is very much reminiscent of the deconfinement transition line of Refs. [2,6], and is suggestive of a merger of the deconfinement transition line with the bulk transition line.

A possible litmus test of the coincidence scenario is to see two separate transitions on the same lattice, especially in the vicinity where the two transition lines meet and remain coincident thereafter. From the transition points in Table I and Fig. 2 one can see that at $\beta_v \sim 0.7$, one may see two separate transitions for $N_\tau = 4$ lattices. Such an expectation was borne out by an explicit study at $\beta_v = 0.7$ on an $8^3 \times 4$ lattice, the results of which are shown in Figs. 5a and 5b. The former, a hysteresis run performed from the low β_f end, shows that all observables, P, P_a and $\langle |L_f| \rangle$ show a jump at around $\beta_f \approx 2.21$ whereas the latter shows the order parameter $\langle |L_f| \rangle$ along with its susceptibility, obtained from the longer run mentioned above. It clearly shows a second order deconfinement transition taking place first at $\beta_f \sim 2.1$, followed by a bulk phase transition later at $\beta_f \sim 2.2$.

We have carried out a similar exercise for $N_\tau = 6$ lattices as well, with essentially similar results. The deconfinement trajectory now starts from the Wilson axis at $\beta_f \approx 2.43$ [17]. At $\beta_v = 0.3$ and 0.5 we get a continuous transition, with the transition point shifted to a slightly higher β_f (see Fig. 2), as expected for a physical transition. The susceptibility curves for $N_\sigma = 12$, 14 and 18 lattices, shown in Fig. 6, and the critical exponent obtained from them, shown in Table II, indicate an Ising - like second order transition at these points. On increasing β_v further, the transition line hits the 1st order line and turns first order, but now at a slightly smaller value of β_v. Already at $\beta_v = 0.7$ one sees a first order transition, as can be seen form the plaquette and Polyakov loop distributions shown in Fig. 7. One thus needs to choose a slightly smaller value of β_v for $N_\tau = 6$ in order to see again two transitions on the same lattice but one does see them. The $\lambda = 1$ simulations for the mixed Villain action thus lend a strong credibility to the hypothesis that the deconfinement transition line for possibly a large range of N_τ merges with the bulk transition line. Since the latter branches out in this case and exhibits no end point, the merger is easy to observe numerically: the small β_v region has only a deconfinement transition line and the large β_f region has only a bulk transition line, while they seem to be coincident in the $\beta_v \gtrsim 0.7$ region.

While the Z_2 - monopole suppression thus provides convincing indications that the un-physical bulk transition line is coincident with the physical deconfinement transition line for a range of N_τ, and thus provides a reasonable explanation for the latter turning first order in the β_f - β_v plane, it is insufficient to remove all the bulk transitions from the region of interest and to show a second order transition similar to the Wilson action case for large β_v values. We therefore turn our attention in the next section to the other Z_2 objects causing the remaining bulk transition : the electric vortices [7].

IV. SUPPRESSION OF ELECTRIC VORTICES
AND MAGNETIC MONOPOLES

In order to suppress the electric vortices in addition to the magnetic monopoles, we consider the action

$$S(U, \sigma) = \beta_f \sum_p \left(1 - \frac{1}{2} \mathrm{Tr}_f U_p \right)$$
$$+ \beta_v \sum_p \left(1 - \frac{1}{2} \sigma_p . \mathrm{Tr}_f U_p \right)$$
$$+ \lambda \sum_c (1 - \sigma_c) + \gamma \sum_l (1 - \sigma_e) , \tag{11}$$

with σ_e defined in Eq. (4). The last term suppresses the Z_2 electric current loops. It should be irrelevant in the continuum limit, leaving the relation between the continuum coupling and β_f and β_v unchanged. For sufficiently large γ, one expects that the bulk transition line caused by the condensation of electric loops will be suppressed. One can reduce the number of input parameters by sending $\lambda \to \infty$ and using the the explicit self-dual form of the above action. The monopole term is then absent and the plaquette variables σ_p are replaced by products over corresponding Z_2 - link variables. This form has the advantage of being more tractable numerically. We employed this self-dual form for our investigations at large γ.

We followed the same procedure as in the previous section to monitor $\langle |L_f| \rangle$ and the finite size scaling behavior of its susceptibility for studying the finite temperature transition. P and P_a were utilized to look for the bulk transitions. We used a heat-bath algorithm for both the gauge and Z_2 variables. One sweep consisted of updating all the gauge variables of the lattice, followed by updating of all the Z_2 variables. We made a number of hysteresis runs of 15000 iterations per point at different β_v values on a $8^3 \times 4$ lattice. No discontinuous transition was found anywhere in the $\beta_v - \beta_f$ plane. The plaquette variables P and P_a were smooth everywhere, indicating that the additional term has succeeded in eliminating all bulk transitions. The deconfinement transition points were estimated from the rise in $\langle |L_f| \rangle$. In order to look for the expected shift in the deconfinement transition point, we repeated the exercise on a $12^3 \times 6$ lattice. Our investigations revealed lines of deconfinement transition points, consistent with (see Fig. 8)

$$\beta_f + \beta_v \approx \beta_c^W , \tag{12}$$

where β_c^W is the deconfinement transition point for the Wilson action (≈ 2.30 for $N_\tau = 4$ [4] and ≈ 2.43 for $N_\tau = 6$ [17] lattices). Rapid but continuous rises of $\langle |L_f| \rangle$, associated with diverging susceptibilities with increasing spatial volume, were found at the deconfinement transitions at all the β_v values investigated. These properties are similar to the known features of the deconfinement transition for the Wilson action for SU(2).

The critical exponent ω was obtained from a finite size scaling analysis of the L_f-susceptibility on $N_\sigma^3 \times 4$ lattices with $N_\sigma = 8$, 12 and 14 at $\beta_v = 1$ and 2. Long simulation runs of 10^5 thermalized configurations and the usual spectral density methods were used to obtain the peak height at the transition point for each lattice. The susceptibility peaks are shown in Fig. 9. For $N_\tau = 6$, we used $N_\sigma = 12$, 14 and 18 and investigated the β_v values 0.5

and 1.5. The results are shown in Fig. 10. Values of the critical exponent ω obtained from these peaks are listed in Table III, and are in good agreement with the value for the Wilson action for SU(2). This behavior is, of course, what one expects from universality arguments. Moreover, the phase transition line, Eq. (12), is also consistent with the expected continuum limit behavior of this action.

Suppressing the artifacts which cause the (first order) bulk transitions in the mixed Villain action, namely, the Z_2 magnetic monopoles and vortices defined above, thus yield results consistent with expectations from universality, both for the order of the transition as well as the shift of the transition point with N_τ. Perturbatively, one expects the contribution of these topological objects to be zero in the continuum limit. It is, however, unclear whether this is indeed so nonperturbatively as well. In fact, the earlier results for the unsuppressed action ($\lambda = \gamma = 0$) suggest that very large N_τ ($\gg 16$) will be needed to see the deconfinement transition separate out from the bulk transition in the β_f - β_v plane.

V. SUMMARY AND CONCLUSIONS

Earlier numerical simulations on asymmetric $N_\sigma^3 \times N_\tau$ lattices using mixed actions, defined by Eq. (1) or (3), yielded apparently paradoxical results. The deconfinement phase transition in these cases was found to become first order for a large range of the adjoint coupling, although one naively expects these actions to be in the same universality class as the Wilson action, which is known to have a second order deconfinement transition. On the other hand, the transition exhibited very little shift with the temporal lattice size N_τ and the average action was also discontinuous at the transition. These results could be consistent with universality if a curious interplay between the physical deconfinement transition and the bulk transitions, which are merely lattice artifacts, existed for some unknown reasons. The absence of any significant variations in the locations of the transition or any change in its nature for large β_v made other options of saving universality rather implausible.

Since variations with N_τ, a defining characteristic of the deconfinement phase transition which is not supposed to affect the bulk transition, failed to resolve the paradoxes, it seemed natural to seek a mechanism to shift or eliminate the bulk transition(s), leaving the universality class intact. Taking a clue from our earlier studies for the SO(3) gauge theory, where a similar mixture of bulk and deconfinement effects is seen, we attempted in this paper elimination of the bulk transition(s) by suppressing certain topological objects as a means to study the deconfinement transition in the mixed theory.

First, we considered the mixed Villain action with an addition of a chemical potential for the Z_2 - magnetic monopoles and studied the phase diagram on asymmetric lattices in the β_f - β_v plane of couplings. The monopoles get suppressed with increasing chemical potential λ. Numerical simulations for $\lambda = 1$ showed an interesting phase diagram which was quite different from that of the original theory. Nevertheless, it still shared the paradoxes mentioned above. We could, however, demonstrate that i) a second order deconfinement transition line emanating from the β_f axis meets the bulk transition line at a finite β_v, ii) the bulk transition line has no end point, and iii) the change of the order of the deconfinement phase transition occurs as the two lines merge. Moreover, we were able to show the presence of two phase transitions on the same finite lattice in the vicinity of the point of merger : a second order deconfinement phase transition, indicated by a continuous sharp rise in the

order parameter, followed by a discontinuous bulk transition, where all observables exhibited an abrupt change, but both sides of the transition were in a deconfined state.

A further suppression of the Z_2 electric vortices enabled us to get rid of the bulk transitions completely, as there was no trace of any discontinuity anywhere in the coupling space and the average plaquette variables were smooth everywhere. A study of deconfinement transition in this theory revealed a line of second order deconfinement transitions, obeying $\beta_f + \beta_v \sim \beta_c^W$, where β_c^W is the corresponding transition point for the Wilson action. Therefore the removal of the bulk transition lines by suppressing the topological objects causing those transitions led to results fully consistent with universality. Since the terms added to the action in the process do not contribute in the naive continuum limit, one can formally attribute the anomalous behavior of the deconfinement transition lines for the action in Eq. (3) to the presence of bulk transitions. Of course, it is natural to expect that the same thing happens for the action in Eq. (1), too. While the vexed possibility of violation of universality in these cases is thus finally eliminated, some nagging questions still remain. Foremost amongst them is how rapidly the topological objects discussed here vanish from the lattice for the original theories as one approaches the continuum limit. Simply put, even for the original theories one now expects for sure the separation of the two lines of transitions for some N_τ. However, it is also clear that it must be at an almost astronomically large value. One knows that this is indeed the case for spin models [18], where one needs to work at a billion times larger correlation lengths to see universal behavior in the adjoint direction. One does not expect it to be so, however, for a continuous gauge symmetric case as ours. Another interesting and related question is about the behavior of the order parameter at the bulk transition when the two transitions do separate : it will have to be continuous and zero through the bulk transition and it will also be exponentially small after the deconfinement phase transition for very large N_τ due to the divergences associated with the point source it represents.

REFERENCES

[1] K. Wilson, Phys. Rev. D **10**, 2445 (1970).

[2] R. V. Gavai, M. Grady and M. Mathur, Nucl. Phys. **B423**, 123 (1994).

[3] G. Bhanot and M. Creutz, Phys. Rev. D **24**, 3212 (1981).

[4] J. Engels, J. Fingberg and M. Weber, Nucl. Phys. B **332**, 737 (1990).

[5] M. Mathur and R. V. Gavai, Nucl. Phys. **B448**, 399 (1995), Phys. Rev. D **56**, 32 (1997).

[6] P. W. Stephenson, `hep-lat`/9604008.

[7] L. Caneschi, I. G. Halliday and A. Schwimmer, Nucl. Phys. **B200**, 409 (1982).

[8] S. Cheluvaraja and H. S. Sharatchandra, `hep-lat`/9611001.

[9] Saumen Datta and R. V. Gavai, Phys. Rev. D **57**, 6618 (1998).

[10] I. G. Halliday and A. Schwimmer, Phys. Lett. **102B**, 337 (1981).

[11] Saumen Datta and R. V. Gavai, Phys. Rev. D **60**, 034505 (1999).

[12] In Ref. [6], a slight shift in the deconfinement transition line was obtained near the end of the bulk line in going from $N_\tau = 4$ to 8, unlike in Ref. [5]. While this shift was interpreted in Ref. [6] as indicating a decoupling of bulk and deconfinement effects at $N_\tau = 8$, in our opinion, it was too small and is more likely to be due to finite size effects. In any case, the $N_\tau = 8$ deconfinement line was also seen to bend towards, and finally merge with, the bulk line. Clearly, there were substantial interference effects of bulk and deconfinement phenomena there too.

[13] R. Savit, Rev. Mod. Phys. **52**, 453 (1980).

[14] E. Fradkin and S. H. Shenker, Phys. Rev. D **19**, 3682 (1979).

[15] R. V. Gavai and M. Mathur, Phys. Lett. B in press, `hep-lat`/9905030.

[16] A. M. Ferrenberg and R. H. Swendsen, Phys. Rev. Lett. **61**, 2635 (1988).

[17] J. Engels, J. Fingberg and D. E. Miller, Nucl. Phys. B **387**, 501 (1992).

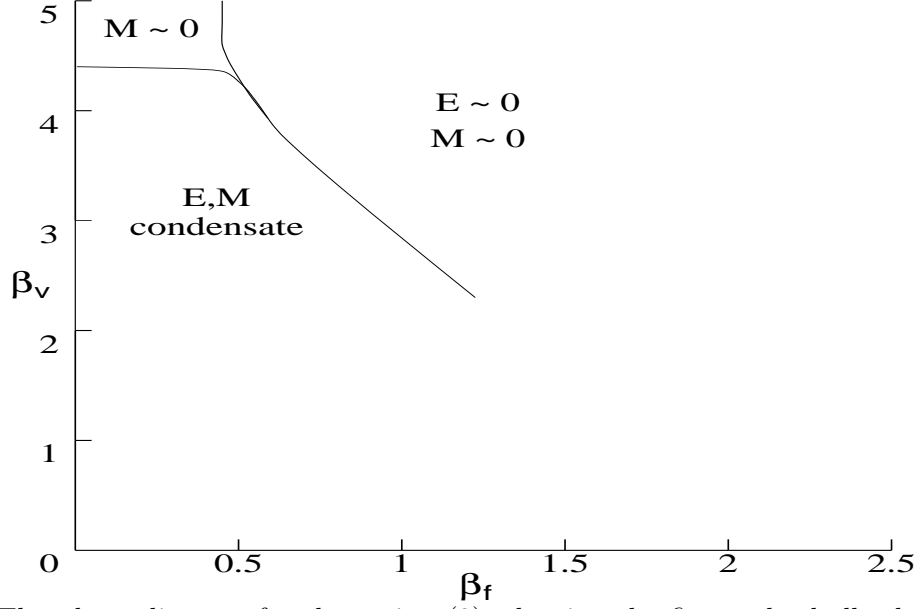[18] M. Hasenbusch, Phys. Rev. D **53**, 3445 (1996).

FIG. 1. The phase diagram for the action (3), showing the first order bulk phase transition lines (from Ref. [6]). The bulk phases are characterized by values of E and M, as shown.
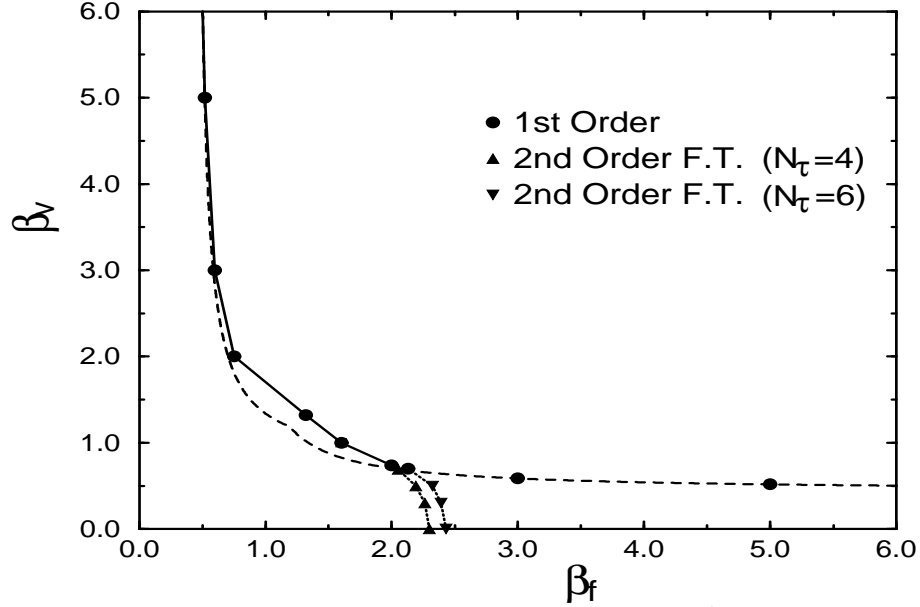

FIG. 2. The phase diagram for the action (5) with $\lambda = 1$ on an $8^3 \times 4$ lattice. The filled circles show first order transition points. The dashed lines show the estimates from Eqs. (6) and (10). The triangles in the low β_v region show the locations of Ising-like second order deconfinement phase transitions on $N_\tau = 4$ and 6 lattices respectively. The dotted and solid lines show the second and first order deconfinement transition lines.

FIG. 3. $\chi_{|L_f|}$ as a function of β_f for $N_\tau = 4$ lattices with $N_\sigma = 8$, 12 and 16 for the action (5) at $\beta_v = 0.7$, 0.5 and 0.3. The values obtained directly from the long simulation runs are also shown with error bars. The lines were obtained using Ferrenberg-Swendsen extrapolation.
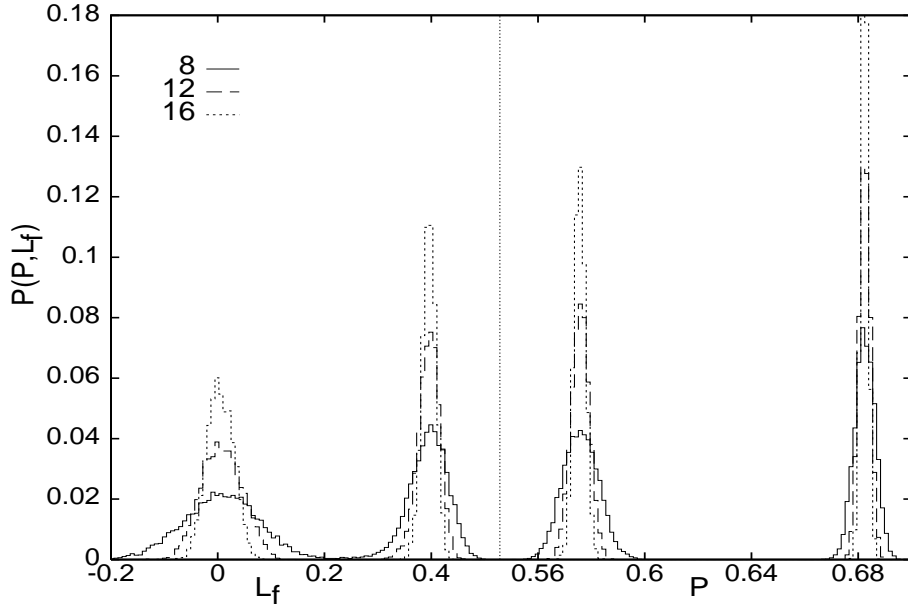

FIG. 4. Probability distributions of L_f and the plaquette variable at $\beta_v = 0.74$, $\beta_f = 2$, for $N_\tau = 4$ lattices with $N_\sigma = 8$, 12 and 16. Two peak structures are visible that sharpen with increase in lattice size, indicating a first order transition. The L_f peaks clearly indicate that the transition is a deconfining one.
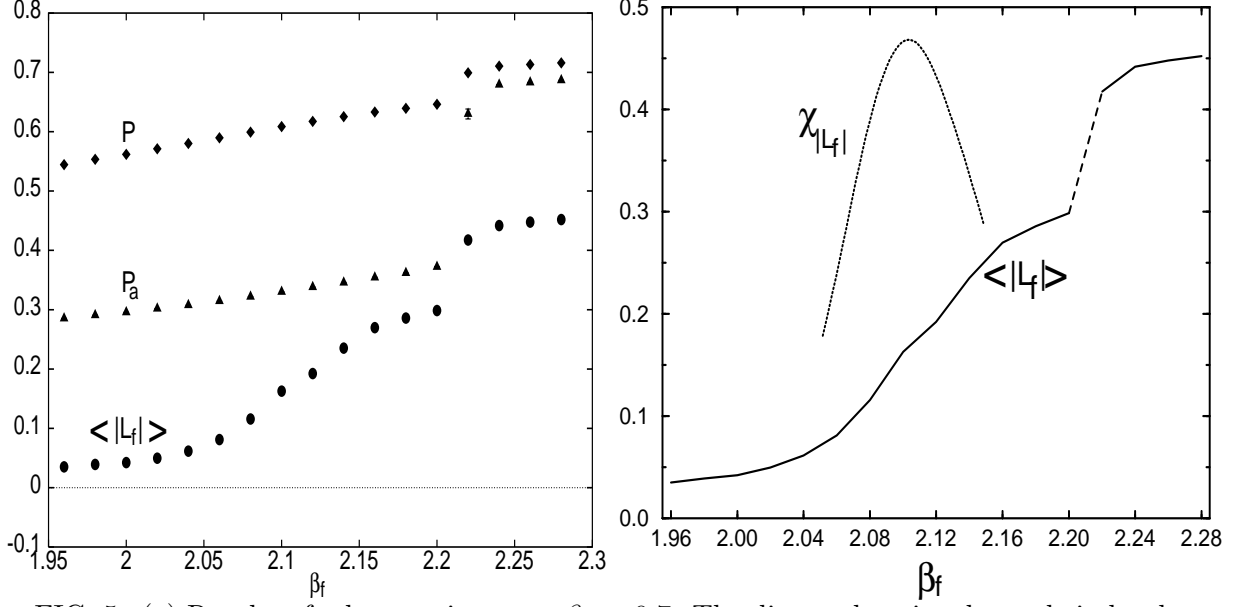
FIG. 5. (a) Results of a hysteresis run at $\beta_v = 0.7$. The diamonds, triangles and circles denote the variables P, P_a and $\langle |L_f| \rangle$ respectively. $\langle |L_f| \rangle$ is seen to rise at $\beta_f \sim 2.1$, and a discontinuous transition is seen at $\beta_f \sim 2.2$. (b) $\langle |L_f| \rangle$ and its susceptibility as a function of β_f at $\beta_v = 0.7$, showing clearly a second order deconfinement transition at $\beta_f \sim 2.1$ and a first order transition at $\beta_f \sim 2.2$.
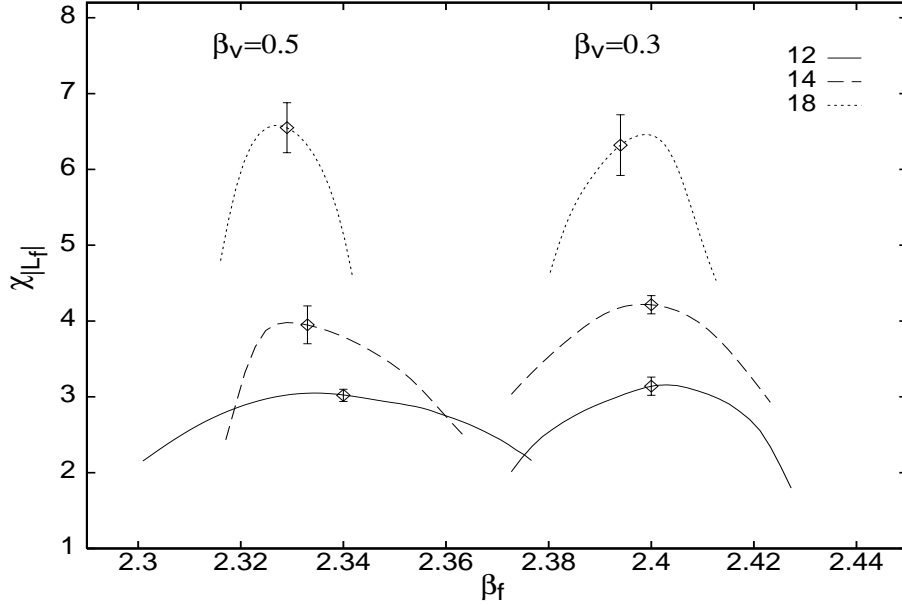

FIG. 6. $\chi_{|L_f|}$ as a function of β_f for $N_\tau = 6$ lattices with $N_\sigma = 12$, 14 and 18, for the action (5) at $\beta_v = 0.5$ and 0.3. The values obtained directly from the long simulation runs are also shown with error bars. The lines were obtained using Ferrenberg-Swendsen extrapolation.
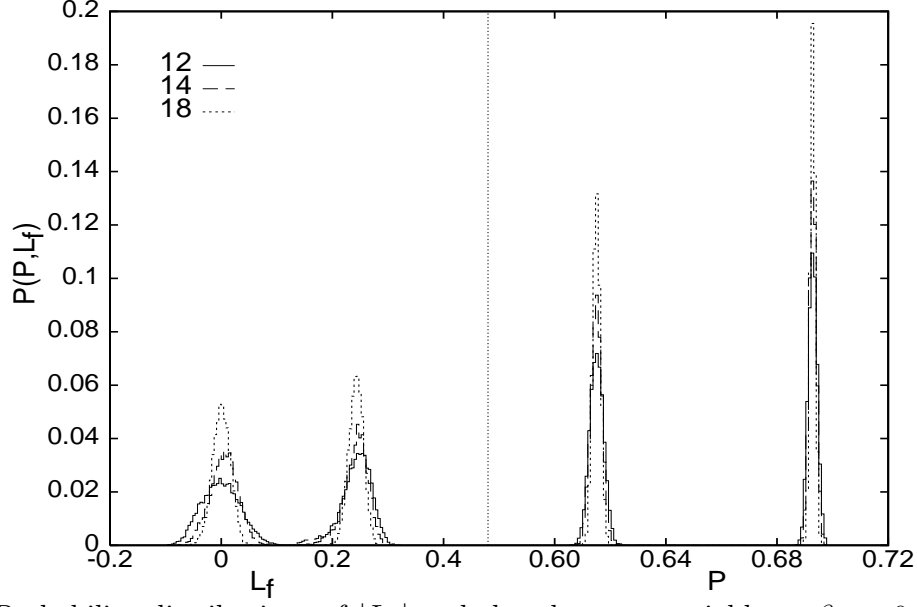
FIG. 7. Probability distributions of $|L_f|$ and the plaquette variable at $\beta_v = 0.7$, $\beta_f = 2.12$ for $N_\tau = 6$ lattices with $N_\sigma = 12$, 14 and 18, showing metastable states indicating a first order transition.
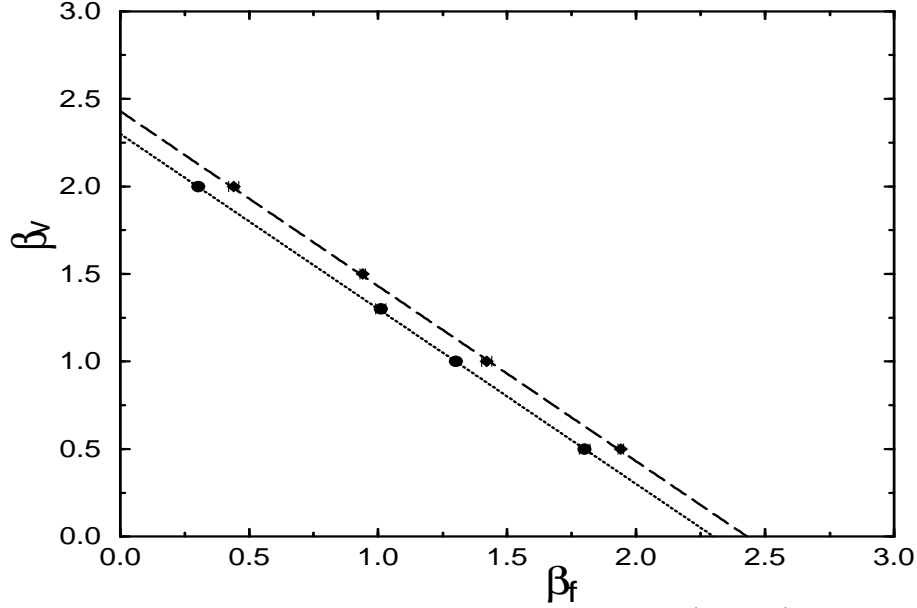

FIG. 8. Locations of the deconfinement transition points in the (β_f, β_v) plane. The circles and diamonds show the simulation points for $N_\tau = 4$ and 6 lattices, respectively. The lines correspond to Eq. (12).
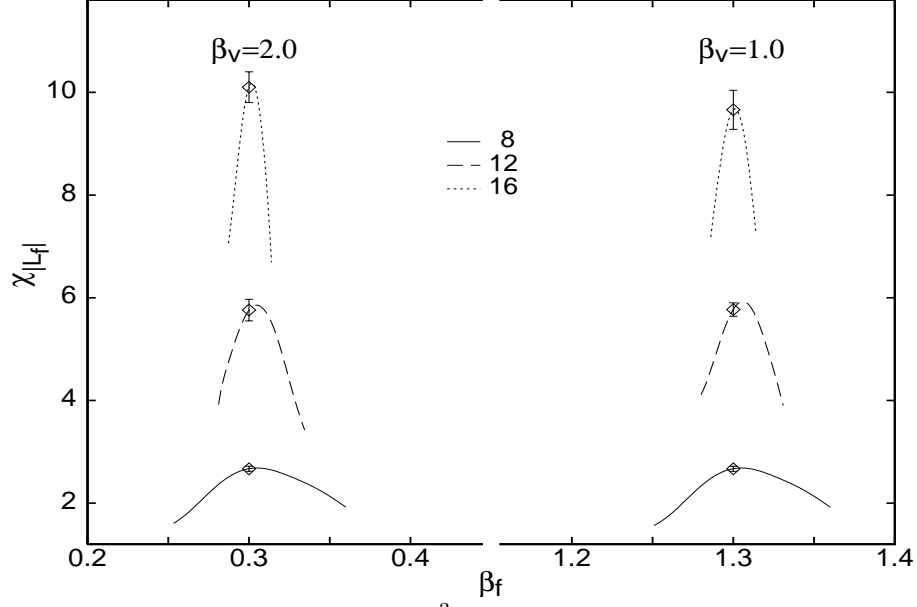
FIG. 9. Polyakov loop susceptibilities for $N_\sigma^3 \times 4$ lattices for $N_\sigma = 8$, 12 and 16, for $\beta_v = 1$ and 2.
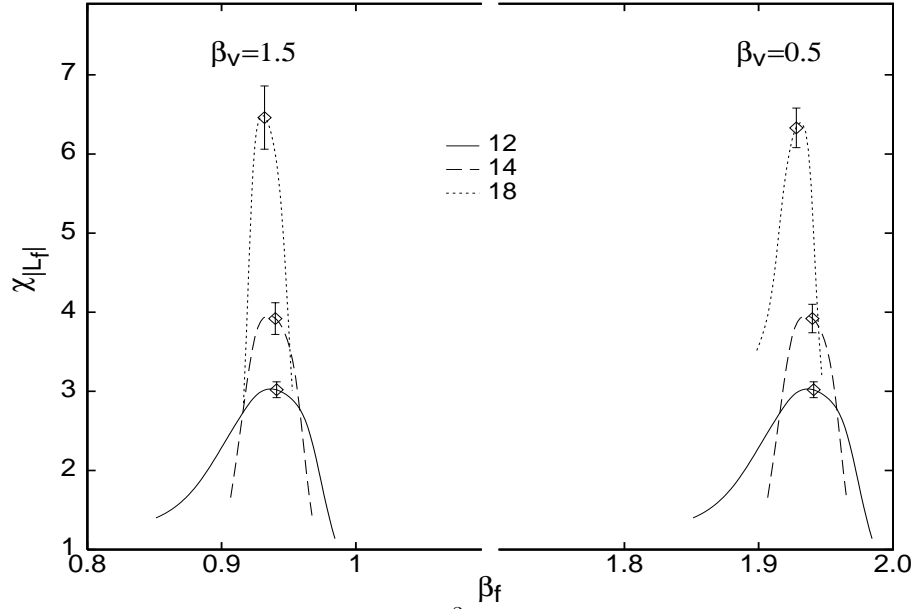

FIG. 10. Polyakov loop susceptibilities for $N_\sigma^3 \times 6$ lattices for $N_\sigma = 12$, 14, 18, for $\beta_v = 0.5$ and 1.5. The errors are shown for the simulation points.

TABLES

TABLE I. Transition points and discontinuities for the first order transitions in the monopole suppressed mixed action.

β_{vc}	β_{fc}	ΔP	ΔP_a	$\Delta \langle |L_f| \rangle$	$|L_f|_-$
5.0	0.52(2)	0.36(2)	0.007(3)	0.60(4)	0.04(3)
3.0	0.60(2)	0.33(2)	0.022(4)	0.46(4)	0.03(2)
2.0	0.76(2)	0.26(1)	0.08(1)	0.38(6)	0.07(5)
1.0	1.60(4)	0.17(4)	0.22(5)	0.35(6)	0.06(4)
0.74(2)	2.0	0.11(1)	0.32(1)	0.33(6)	0.05(4)
0.59(2)	3.0	0.023(4)	0.33(2)	0.04(5)	0.51(4)
0.52(2)	5.0	0.007(2)	0.36(2)	0.01(6)	0.69(4)

TABLE II. Values of the critical index ω for the monopole suppressed action.

	$N_\tau = 4$			$N_\tau = 6$	
β_v	0.3	0.5	0.7	0.3	0.5
ω	1.92 ± 0.05	1.87 ± 0.05	1.91 ± 0.02	1.82 ± 0.08	1.89 ± 0.07

TABLE III. Values of the critical index ω for the action with both monopoles and vortices suppressed.

	$N_\tau = 4$		$N_\tau = 6$	
β_v	1.0	2.0	0.5	1.5
ω	1.88 ± 0.05	1.93 ± 0.05	1.84 ± 0.06	1.86 ± 0.07